Toxicon 251 (2024) 108152

Contents lists available at ScienceDirect

Toxicon

journal homepage: www.elsevier.com/locate/toxicon

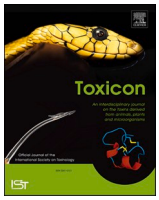

Azaspiracid-59 accumulation and transformation in mussels (*Mytilus edulis*) after feeding with *Azadinium poporum* (Dinophyceae)

Bernd Krock [a,*], Elizabeth M. Mudge [b], Annegret Müller [a], Stefanie Meyer [c], Jan Tebben [a], Pearse McCarron [b], Doris Abele [c,1], Urban Tillmann [a]

[a] Alfred-Wegener-Institut Helmholz-Zentrum für Polar und Meeresforschung, Ökologische Chemie, Bremerhaven, Germany
[b] Biotoxin Metrology, National Research Council of Canada, Halifax, NS, B3H 3Z1, Canada
[c] Alfred-Wegener-Institut Helmholz-Zentrum für Polar- und Meeresforschung, Benthosökologie, Bremerhaven, Germany

ARTICLE INFO

Handling editor: Ray Norton

Keywords:
Biotransformation
AZA variants
LC-MS/MS
Esterification
Shellfish

ABSTRACT

Azaspiracid-59 (AZA-59) was detected in plankton in coastal waters of the Pacific Northwest USA. Given that bivalves metabolize and transform accumulated phycotoxins, a strain of *Azadinium poporum* isolated from the coast of Washington State that is a known producer of AZA-59 was used in a controlled feeding experiment with mussels (*Mytilus edulis*) to assess AZA-59 accumulation rates and transformation into shellfish metabolites. Mussels started feeding immediately after the addition of *A. poporum*. Mussels were generally healthy during the entire experimental exposure of 18 days with prevailingly high rates of clearance (approx. 100 mL per mussel per hour) and ingestion. Mussels were extracted after different exposure times and were analyzed by liquid chromatography coupled with low- and high-resolution mass spectrometry. In the course of the experiment a number of putative AZA-59 metabolites were detected including hydroxyl and carboxy analogues that corresponded with previously reported mussel metabolites of AZA-1. A significant formation of 3-OH fatty acid acyl esters relative to free AZAs was observed through the time course of the study, with numerous fatty acid ester variants of AZA-59 confirmed. These results illustrate the potential for metabolism of AZA-59 in shellfish and provide important information for local AZA monitoring and toxicity testing along the Northern Pacific US coast.

1. Introduction

Azaspiracid shellfish poisoning (AZP) is a human syndrome that was reported for the first time in 1996 caused by mussels contaminated with azaspiracids (AZAs) (McMahon and Silke, 1996). The biological origin of AZA was initially unknown, but due to their chemical structures belonging to the polyketide group, AZA were suspected to be of microalgal origin (James et al., 2000). Later the dinoflagellate *Azadinium spinosum*, which until that time had been unknown, was described and identified as the source of AZA-1 and -2 (Krock et al., 2009; Tillmann et al., 2009). In the following years more AZA-producing species and AZA variants were found (Kilcoyne et al., 2014; Kim et al., 2017; Krock et al., 2014, 2015, 2019; Rossi et al., 2017; Tillmann et al., 2017). In addition to the *de novo* biosynthesized AZA variants the total number of reported AZA analogues is additionally amplified by metabolic activity of filter-feeding bivalves that accumulate and biotransform the ingested AZAs (Kilcoyne et al., 2018; Salas et al., 2011).

AZA profiles in the field depend on the producing species present, but even within an AZA-producing species, there are geographically distinct patterns (Krock et al., 2014, 2019; Tillmann et al., 2018). For example, in Argentine waters *Azadinium poporum* AZA profiles are dominated by AZA-2 (Ramírez et al., 2022; Tillmann et al., 2016), and in *A. poporum* from the North Pacific US coast the predominant variant is AZA-59 (Kim et al., 2017). The discovery of an AZA producing *A. poporum* in North America is significant, especially considering the recent structural confirmation and demonstration of equivalent relative toxicity to AZA-1 (Tebben et al., 2023). Given that the AZA-59 producing *A. poporum* was originally isolated from the region of Puget Sound (Washington State), a clear objective is to describe the accumulation rate of this toxin and potential metabolic products. Bivalves are abundant in the region and include many different species such as manila clam (*Ruditapes philippinarum*), razor clam (*Siliqua patula*), as well as

* Corresponding author.
E-mail addresses: bernd.krock@awi.de (B. Krock), Elizabeth.Mudge@nrc-cnrc.gc.ca (E.M. Mudge), annegret.mueller@awi.de (A. Müller), stefanie.meyer@awi.de (S. Meyer), jan.tebben@awi.de (J. Tebben), Pearse.McCarron@nrc-cnrc.gc.ca (P. McCarron), urban.tillmann@awi.de (U. Tillmann).
[1] Deceased November 21, 2021.

https://doi.org/10.1016/j.toxicon.2024.108152
Received 22 July 2024; Received in revised form 9 October 2024; Accepted 23 October 2024
Available online 26 October 2024

mussels (e.g., *Mytilus trossulus*) and oysters (e.g., *Crassostrea* spp.) (Trainer and King, 2023). In total, the bivalve shellfish produced in Washington State exceeds USD 150 million per year (USDA, 2013). Little is known on the concentration or profiles of toxins in different species of locally abundant bivalves, let alone accumulation rates and metabolic products. Consequently, we chose *Mytilus edulis* as our model species for this study in order to produce data that are comparable with studies on the metabolic products of other AZAs (see (Kilcoyne et al., 2018; Salas et al., 2011)).

The aim of this work was to investigate feeding of blue mussels (*M. edulis*) on AZA-59 producing *A. poporum*, with a specific focus on the accumulation and biotransformation of AZA-59 in the mussels.

2. Materials and methods

2.1. Azadinium poporum *culture conditions*

Azadinium poporum strain 121-E10, which was isolated from Puget Sound in 2016 (Kim et al., 2017), was grown at 15 °C in a natural seawater medium prepared with sterile-filtered (0.2 μm VacuCap filters, Pall Life Sciences, Dreieich, Germany) North Sea (salinity: 34, pH adjusted to 8.0) and enriched with 1/10 strength K-medium (Keller et al., 1987), slightly modified by replacing the organic phosphorus source by 3.62 μM Na_2HPO_4 and by omitting the addition of ammonium ions. The strain was grown in 10 L glass bottles at 15 °C under a photon flux density of 70 μmol m^{-2} s^{-1} on a 16:8 h light:dark photocycle. Cell density was determined by settling Lugol's fixed samples and counting >400 cells under an inverted microscope (Axiovert 200M, Zeiss, Göttingen, Germany).

To assess the amount of AZA in the shellfish feeding experiments, AZA cell quota of each *A. poporum* culture used as food were determined in triplicates (Table S1). Previous AZA quantification for laboratory culture had shown that AZAs are clearly intra-cellular with >90% of toxins in the particulate fraction (Jauffrais et al., 2012b) (own unpublished results) and therefore AZA content of the cell pellet but not of the cell-free supernatant was determined. A 50 mL aliquot was harvested by centrifugation at 894×*g* for 15 min (5810R, Eppendorf, Hamburg, Germany). After centrifugation, supernatants were discarded and cell pellets were mixed with 300 μL acetone, each and frequently stirred within 1 h. The suspensions were filtered over 0.45 μm centrifugation filters (Ultrafree, Millipore, Eschborn, Germany) for 60 s at 5000×*g* (5424R, Eppendorf). The samples were transferred into conical HPLC vials and volumes adjusted to 250 μL. Samples were stored at −20 °C until analysis of AZA cell quota.

2.2. Experimental setup

Mussels (*Mytilus edulis*) were collected on the beach of the island Sylt, Germany and were transported to AWI, Bremerhaven in April 2018. Mussels were acclimated in North Sea water (salinity of 34) at 15 °C in a 15-L aquarium for a week before starting the experiment. During this period mussels were fed every two days with the algae *Nannochloropsis* (1.2×10^5 cells mL^{-1}). In addition, nutrient concentrations of aquarium water (ammonium, nitrite, nitrate) were monitored in three-day intervals with a nutrient analyzer (QuAAtro, Seal Analytical, Norderstedt, Germany) and in case of threshold exceedance (>0.4 mg L^{-1} ammonium, >0.2 mg L^{-1} nitrite, and >50 mg L^{-1} nitrate) the aquarium water was exchanged.

2.2.1. Main experiment

Before starting the main experiment, 12 mussels (5–6 cm length) were placed in each of four 15 L aquaria with 10 L North Sea water and aquaria were aerated by bubbling the water with air. Mussels were starved for one week and nutrients were monitored as before and water was exchanged in case one nutrient exceeded the above-mentioned threshold levels. One of the four aquaria was designated as the control group, whereas the remaining three aquaria were designated as replicate feeding treatments.

At T = 0 of the main experiment, three mussels of each treatment were harvested at the beginning of the experiment and subsequently food cultures were added to achieve 120×10^3 cells mL^{-1} of *Nannochloropsis* (one control) or 5×10^3 cells mL^{-1} of *A. poporum* (triplicate experimental aquaria). During the first 12 h, samples for algal cell counts were taken after 1, 3, 6, 9, and 12 h and fixed with Lugol's solution (1 % final concentration). Thereafter, cell count samples were taken at 18, 33, 36, 42, 57, 60, 66, 81, and 84 h. Experimental and control aquaria were spiked with additional food after 12, 36 and 60 h. Therefore, a precalculated amount of aquarium water was removed and replaced by stock cultures of *A. poporum* or *Nannochloropsis* to reach 5×10^3 or 120×10^3 cells mL^{-1}, respectively. All microalgal cell density estimates were performed by cell counts as described above. After 12, 36 and 84 h, three mussels from each experimental and control aquarium were harvested resulting in 12 animals at each time point across all replicates. On every sampling occasion a fitness test was performed with all mussels with open shells by stimulating the visible mantle with a needle. Mussels that reacted with shell closure were regarded as fit and healthy. After harvest the entire mussels were weighed and thereafter the soft tissue was removed and weighed. Finally, the hepatopancreas (without the style) was separated and weighed. In addition, the length, width and height of the shells were measured and shells were weighed (Table S2). All soft tissues were frozen at −20 °C until extraction.

To account for potential effect of experimental conditions (aeration, light etc.) on potential growth or decline of *A. poporum*, a single control experiment was performed in parallel to the main experiment. Therefore, a 500 mL Erlenmeyer flask was filled with 300 mL of *A. poporum* at 5×10^3 cells ml^{-1}, which was aerated as the aquaria and which was sampled at the same frequency as the experimental containers.

2.2.2. Prolonged exposure experiment

At the end of the main experiment a total of 8 mussels remained. To investigate mussel behavior and AZA metabolism upon prolonged exposure to the *A. poporum* strain, these eight mussels were combined and further incubated in one 15 L aquarium filled with 10 L North Sea water as described above, which was initially (corresponding to 86 h after starting the main experiment) adjusted to 10×10^3 cells mL^{-1} of *A. poporum*. An *A. poporum* control (one aerated 250 ml Erlenmeyer) was set up as well. Cell count samples were then taken after 90, 138, 210 and 258 h. At 138 h new *A. poporum* food was added to roughly restore of food density of 10×10^3 cells mL^{-1}. At t = 258 h, 5 mussels were harvested. For the remaining three mussels, long-term AZA-59 exposure was continued (starting at T = 288 h) by exposing these 3 mussels in a 2 L aerated Erlenmeyer with 1.5 L seawater spiked with *A. poporum* at 12×10^3 cells mL^{-1}. A new *A. poporum* control (200 mL aerated Erlenmeyer, which was replaced by a new control after 378 h) was set up in parallel. The exposure lasted for additional 138 h, with cell count samples taken at irregular intervals, and with restoration of high food densities of about 16×10^3 cell mL^{-1} by replacing water with new algal culture after 332 and 372 h, respectively. The whole experiment was terminated on day 18 (426 h) by harvesting the remaining 3 mussels.

2.3. Calculation of filtration rate

Control set up of *A. poporum* without mussel did not significantly change over time and consequently calculation of ingestion and filtration rates did not consider intrinsic growth or mortality of *A. poporum* during the feeding intervals. Filtration rate or clearance f (mL per mussel per hour) and ingestion I (cells eaten per mussel per hour) was thus calculated according to Frost (1972) as

$$f = \frac{V \bullet (\ln C_0 - \ln C_1)}{n \bullet t}$$

with V being the aquarium volume (in mL), C_0 and C_1 the *A. poporum* cell densities at the beginning and the end of the period under consideration, n the number of mussels, and t the duration of the period in hours. Ingestion was then calculated as

$$I = \frac{(C_0 - C_1) \bullet V}{n \bullet t}$$

2.4. Sample extraction

2.4.1. Hepatopancreas

The individual hepatopancreas of each mussel was removed, lightly blotted dry and weighed, and then transferred to a 2 mL cryovial. To each sample, 0.9 g of ceramic beads (Matrix D, Thermo-Savant, Illkirch, France) and 5 mL of methanol were added and samples were homogenized in FastPrep instrument (Thermo-Savant) for 45 s at 6.5 m s^{-1}. The homogenized samples were centrifuged at 16,100×*g* for 15 min and supernatants transferred to glass vials. This procedure was repeated twice with 500 μL methanol and extracts were combined and dried under a gentle stream of nitrogen. The dry samples were resuspended in 250 μL acetone and the samples filtered over 0.45 μm centrifugation filters (Ultrafree, Millipore, Eschborn, Germany) for 30 s at 6000×*g*. The samples were transferred in to conical HPLC vials and the glass vials were rinsed twice with 250 μL acetone each and spin-filtered as described above. All samples were stored at −20 °C until analysis. In addition, three samples of mussel flesh without hepatopancreas were extracted (for method details see supplementary Table S2).

2.4.2. Extraction of residual AZA

To account for residual AZA other than in the mussel HPs, various samples were taken at the end of the main experiment after 84 h. To account for particulate residuals (remaining *Azadinium* cells, debris, fecal material etc.) water from each of the three experimental aquaria was well mixed and three replicated 50 mL subsamples were harvested by centrifugation (Eppendorf 5810R, Eppendorf, Hamburg, Germany; 3220 g, 10 min). Each pellet was transferred to a microtube, and again centrifuged (Eppendorf 5415; 16,000×*g*, 5 min). The dry cell pellets were mixed with 250 μL acetone and frequently stirred within 1 h. The suspensions were filtered over 0.45 μm centrifugation filters (Ultrafree, Millipore, Eschborn, Germany) for 60 s at 5000×*g* (5424R, Eppendorf). The samples were transferred in to conical HPLC vials and volumes adjusted. Samples were stored at −20 °C until analysis. The corresponding supernatants of the 50 mL aliquots of each aquarium were taken to test for dissolved AZA. The aliquots were loaded on LC-C18 SPE cartridges (Supelclean no. 57054 LC-18, 6 mL tube; Supelco, Deisenhofen, Germany) after activation with 2 mL methanol and subsequent conditioning with 2 mL seawater. The cartridges were de-salted by washing with 3 mL deionized water and AZA were eluted with 5 mL methanol. Samples were taken to dryness under a gentle nitrogen stream and residues re-dissolved in 250 μL. The extracts were filtered through centrifugal filters and filtrates transferred to HPLC vials as described above.

Additionally, the water of each treatment (approx. 16 L) was partitioned into two 10 L carboys and to each carboy 1 g L^{-1} HP20 (Diaion, order no.: 13067, Sigma-Aldrich, Taufkirchen, Germany) and 600 mL acetone (7% final concentration) were added. The water was stirred for 5 five days with a magnetic bar. The two mixtures of the same aquarium were poured over a 50 μm mesh, the retained HP20 was desalted by rinsing several times with deionized water and subsequently dried overnight in an oven at 50 °C. Dry HP20 was transferred into 50 mL centrifugation tubes, 30 mL methanol were added, and gently shaken overnight on a shaker (LS-5, Gerhardt, Königswinter, Germany). The mixture was transferred into a 70 mL glass column and the centrifugation tube was rinsed with 15 mL methanol that was added to the glass column. The column was eluted with additional 25 mL methanol (total volume approx. 60 mL). All column eluates were collected in a 100 mL round flask and the sample was reduced to ca. 1.5 mL in a rotary evaporator. The residue was filtered through 0.45 μm centrifugation filters (Ultrafree), the filtrate dried in a gentle nitrogen stream, re-dissolved in 250 μL acetone, and stored at −20 °C until analysis.

2.5. LC-MS/MS measurements

Water was deionized and purified (Milli-Q, Millipore, Eschborn, Germany) to 18 MΩ cm or better quality. Formic acid (90%, p.a.), acetic acid (96%, p.a.) and ammonium formate (98%, p.a.) were from Merck (Darmstadt, Germany). The solvents, methanol and acetonitrile, were high performance liquid chromatography (HPLC) grade (Merck).

2.5.1. Selected reaction monitoring (SRM)

The analytical system consisted of an API 4000 Q Trap triple quadrupole mass spectrometer equipped with a TurboSpray® interface (Sciex, Darmstadt, Germany) coupled to a model 1100 LC (Agilent, Waldbronn, Germany). The LC equipment included a solvent reservoir, in-line degasser (G1379A), binary pump (G1311A), refrigerated autosampler (G1329A/G1330B), and temperature-controlled column oven (G1316A).

Separation (5 μL sample injection volume) was performed by reverse-phase chromatography on a C8 phase. The analytical column (50 × 2 mm) was packed with 3 μm Hypersil BDS 120 Å (Phenomenex, Aschaffenburg, Germany) and maintained at 20 °C. The flow rate was 0.2 mL min^{-1} and gradient elution was performed with two eluents, wherein eluent A was water and B was acetonitrile/water (95:5 v/v), and both contained 2.0 mM ammonium formate and 50 mM formic acid. The initial conditions were 8 min column equilibration with 30% B, followed by a linear gradient to 100% B in 8 min, isocratic elution until 18 min with 100% B, and then returning to the initial conditions until 21 min (total run time: 29 min).The AZA profiles were determined in one period (0–18 min) with curtain gas: 10 psi, CAD: medium, ion spray voltage: 5500 V, ambient temperature; nebulizer gas at 10 psi, auxiliary gas was off, the interface heater was on, the declustering potential of 100 V, the entrance potential of 10 V, and the exit potential of 30 V. The SRM experiments were carried out in positive ion mode by selecting the transitions shown in Table S3. AZA were calibrated against an external standard solution of AZA-1 (certified reference material from the National Research Council, Halifax, Canada) and estimated as AZA-1 equivalents.

2.5.2. Precursor ion experiments

Precursor ion experiments of the characteristic AZA-59 fragment *m/z* 362 were performed in order to detect potentially not hypothesized AZA-59 variants in the mussel feed experiment. Precursors of *m/z* 362 were scanned in the positive-ion mode from *m/z* 500 to 1000 using the conditions described above for SRM experiments with a collision energy of 70 V and an exit potential of 12 V. Collision induced dissociation (CID) spectra of the *m/z* values 828, 846, 860, 862, 876, 878, 890, and 892 were recorded in the Enhanced Product Ion (EPI) mode in the mass range from *m/z* 150 to 930. Positive ionization and unit resolution mode were used. The MS parameters described above for SRM experiments were used with a collision energy spread of 0, 10 V, a collision energy of 70 V, and an exit potential of 12 V.

2.5.3. High resolution mass spectrometry (HRMS) of AZA analogues

LC-HRMS analysis was performed after Krock et al. (2019) with a Vanquish UPLC system coupled to a Q Exactive Plus mass spectrometer, using a heated electrospray ionization source (Thermo Fisher Scientific). Separation was performed on a C18 column (C18 BEH, 100 × 2 mm, 1.7 μm, equipped with guard-column, Waters) with a flowrate of 0.45 mL min^{-1} and the following binary gradient: Solvent A = 0.1% formic acid in ultrapure water, solvent B = 0.1% formic acid in acetonitrile; after injection, the samples were eluted isocratically at 10% B for 0.5 min, followed by a 6.5 min gradient to 99% B and held for 2.9 min. The

re-equilibration phase at 10% B was 1 min. The effluent of the first 0.5 min was diverted to waste to limit salt deposits. The column oven was set to 40 °C. Data dependent mode with a full scan resolution of 70,000 (*m/z* 200) and scan range *m/z* 810 to 895 followed by five data-dependent acquisition ($ddMS^2$) experiments (normalized collision energy of 35, automatic gain control target of 2×10^5, 50 ms maximum injection time, 0.4 *m/z* isolation window, 1.6×10^3 intensity threshold) was used. For all experiments, the transfer capillary temperature was set to 275 °C, the auxiliary gas heater to 450 °C, the spray voltage was 3.5 kV, the sheath gas flow rate was 55 and auxiliary gas rate 15. The instrument was calibrated with the positive Ion Calibration Solution (Velos, Pierce, Thermo Fisher, Germany).

2.5.4. High resolution mass spectrometry (HRMS) of AZA fatty acid esters

The LC-HRMS method for AZA-esters was adopted from Mudge et al. (2020) with some modifications. In summary, analyses were performed using an Agilent 1200 LC equipped with a binary pump, temperature controlled autosampler and column compartment coupled to a Q Exactive HF Orbitrap mass spectrometer (Thermo Fischer Scientific, Waltham, MA, USA) with a heated electrospray ionization probe (HESI-II). The chromatographic separation used a C8 column (100 × 2.1, 1.9 µm Thermo Hypersil Gold; Thermo Fischer Scientific) with gradient elution. The mobile phase was water (A) and 95% MeCN (B), both containing 50 mM formic acid and 2 mM ammonium formate. The elution gradient (0.25 mL min^{-1}) was: 0–5 min, 50–100% B; 5–25 min, 100% B; 25–25.1 min, 100–50% B; and 8 min re-equilibration at 50% B. The column and sample compartments were maintained at 20 °C and 10 °C, respectively. The three mussel hepatopancreas tissue extracts pertaining to each sample were provided as dried extracts and were dissolved in 250 µL of methanol, combined in 1.0 mL volumetric flasks and made to the mark with methanol. The injection volume of the combined hepatopancreas extracts for each mussel tissue was 3 µL.

The MS was calibrated from *m/z* 74–1622 according to the manufacturer's specification using the positive Pierce LTQ Velos calibration solution (Thermo-Fisher Scientific). Full scan data were collected from *m/z* 750–1250 using positive ionization with a spray voltage of 3.0 kV. The sheath gas pressure was 35 psi and auxiliary gas flow was 10 (arbitrary units). The capillary temperature was 350 °C and the heater temperature was 300 °C. The MS resolution setting was 60,000 with an AGC target of 1×10^6 and a maximum injection time of 100 ms. All Ion Fragmentation (AIF) was used to screen for AZA ester product ions. Full scan spectra were acquired as described above, while AIF was alternatively cycled from a mass range of *m/z* 100 to 1200 with a collision energy of 80 eV. The MS resolution was set at 120,000 with an AGC target of 3×10^6 and a maximum injection time of 200 ms.

$ddMS^2$ was used to collect product ion spectra of the five most abundant ions in the full scan acquisition with a loop count of 5, with an inclusion list for candidate AZA-59 fatty acid esters and AZA-59 metabolite fatty acid esters. The mass range for full scan acquisition was *m/z* 750–1250 with a resolution setting of 60,000, an AGC target of 1×10^6 and maximum injection time of 100 ms. Product ion scans were acquired with an isolation window of 1 *m/z* with a collision energy of 80 eV. The resolution was set to 60,000 with an AGC target of 5×10^5 and a maximum injection time of 100 ms.

3. Results and discussion

3.1. Mussel feed and fitness

3.1.1. Mussel feed

Mussels started feeding immediately after the addition of food, with the algal density declining by approximately 20% after 1 h incubation (Fig. 1A and B). For the single non-toxigenic control *Nannochloropsis*, cell density declined from 130 to 50 × 10^3 cells mL^{-1} after 12 h. *A. poporum* density also continuously decreased from 5.0 × 10^3 cells mL^{-1} to 1.5 × 10^3 cells mL^{-1} after 12 h, at which point mussels were

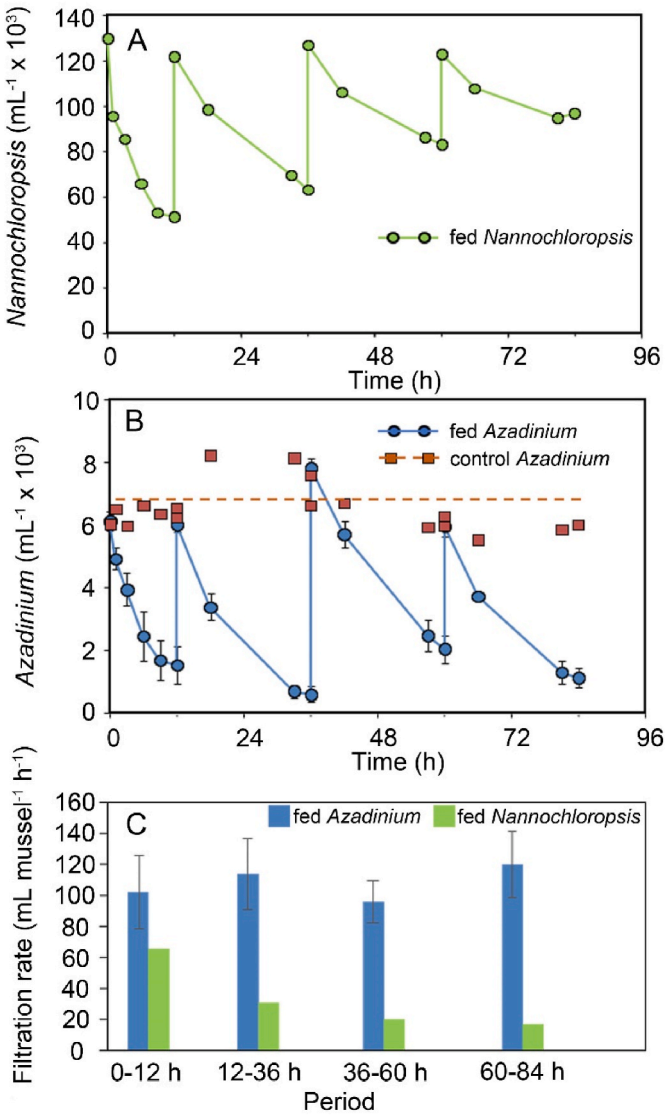

Fig. 1. Cell density changes of *Nannochloroppsis* (n = 1) (A), *A. poporum* (n = 3) (B) and corresponding filtration rates during the main experimental period (C).

harvested from each treatment. After each addition of new *A. poporum* culture over the course of the experiment, cell density declined exponentially. For the *Nannochloropsis* control, the algal density remaining 24 h after food addition increased over the course of the experiment (Fig. 1A). Cell densities of *A. poporum* in the single control (without mussels) did not change significantly (Fig. 1B), indicating that changes in cell density were due to mussel activity. Filtration rate in the *A. poporum* treatment, which was separately calculated for the three periods of food addition, was constant ranging from 94 to 116 mL per mussel per hour (Fig. 1C). Filtration rates of mussels fed with *A. poporum* were higher compared to filtration rates obtained with *Nannochloropsis*, which ranged from 20 to 60 mL per mussel per hour, which declined during the course of the experiment (Fig. 1C).

During the second phase of prolonged *A. poporum* exposure (day 4–11, Fig. S1), the mussels continued to filter and clear the water after each addition of *A. poporum* (Fig. S1A), and the same behavior was observed in the final exposure period from days 12–18 (Fig. S1A). The *A. poporum* control culture in the second phase (day 4–11) slightly decreased with time, but for the final period *A. poporum* cell densities in the control did not significantly change between days 12 and 16, and after the addition of new food at day 16 (Fig. S1A). Filtration rates (clearance) of approximately 100 mL per mussel per hour in the second

phase (day 4–11; Fig. S1B) corresponded to values calculated for the main experiment. Filtration rates for the final phase (day 12–18), where 3 mussels were incubated in an Erlenmeyer flask, were slightly lower and ranged from 20 to 60 mL per mussel per hour (Fig. S1B). The corresponding ingestion rates during the whole experimental period ranged from 0.12 to 0.43 × 10^6 *A. poporum* cells per mussel per hour (Table S4). With these ingestion rates the total amount of *A. poporum* cells removed by each mussel for the respective sampling time increased from 3.8 × 10^6 cells (for mussels harvested after 12 h) to 80 × 10^6 cells for mussels harvest at the end of the whole experiment (after 17 days, 426 h) (Table 1).

3.1.2. Mussel fitness

Mussel viability was tested with individuals fed *Nannochloropsis* (control) in comparison with *A. poporum*. Fitness tests could only be performed on mussels that remained open upon careful removal from the aquarium. The percentage of closed individuals for the control were 100% on day one (n = 12) indicating that they were not filtering at this moment, 56% on day two (n = 5) and 86% on day three (n = 6). The percentage of closed individuals for the *A. poporum* exposed mussels were 97% on day one (n = 35), 34% on day two (n = 9) and 52% on day three (n = 9). The remaining control individuals for the fitness test were 0 (day one), 4 (day two) and 1 (day three) of the control mussels, and 1 (day one), 17 (day two) and 8 (day three) of the *A. poporum* exposed mussels. The only mussels that did not respond to the prick test (i.e., unfit individuals) were found in the group of AZA-treated individuals (two or 12 % for day two and one or 12% for day three), but they reacted later in the experiment.

M. edulis readily ingested *A. poporum* immediately after addition of the algae, as has been observed in previous shellfish feeding studies with *A. spinosum* (Jauffrais et al., 2012a, 2012c; Salas et al., 2011) or *A. poporum* (Ji et al., 2018). In the present study, high rates of clearance/ingestion prevailed through the whole experimental exposure of 18 days. In contrast, Jauffrais et al. (2012a) showed that *A. spinosum*, after a rapid initial AZA accumulation in *Mytilus*, negatively affected mussel feeding behavior causing lower clearance compared to when fed *Isychrysis* control food. During the present experiment, the mussels were generally healthy with only one dead individual, which was excluded. Of the remaining 36 individuals three showed a limited response to pricking with a needle. It is noteworthy that despite exponential decrease of algal abundances in the aquaria, many mussels (including those fed with *Isychrysis galbana*) were closed at the control time points, indicating that observations of the feeding status of the mussels once per day were not representative and did not reflect the actual feeding behavior of individuals during the entire experiment (Ji et al., 2018).

3.2. Mussel metabolites of AZA-59

In order to evaluate the uptake and metabolism of AZA-59, the hepatopancreas tissues, which are known to accumulate higher concentrations of lipophilic toxins, were harvested from mussels exposed to *A. poporum* over the course of the experiment. These were screened by liquid chromatography tandem mass spectrometry (LC-MS/MS) using selected reaction monitoring (SRM) mode with hypothetical mass transitions deduced from the AZA metabolism scheme presented by Kilcoyne et al. (2018). However, the hypothetical metabolism scheme of AZA-59 is less complex than that reported for AZA-1. Hydroxylation at C-3 is one of the reported metabolic reactions reported for AZAs in mussels, but AZA-59 already possesses a 3-hydroxy group and also contains a saturated double bond at C7-C8 (Kim et al., 2017) (Fig. 2). On the other hand, the primary reported location for fatty acid esterification is at the 3-hydroxy group (Mudge et al., 2020), which is present in AZA-59 and thus provides a potential esterification location that is only possible with 3-hydroxy metabolites of AZA-1 that usually are not in high abundance.

The other reported metabolic reactions that AZA-1 and AZA-2 undergo in mussels, specifically C23-hydroxylation, C23-hydroxy oxidation, C22-methyl oxidation and decarboxylation as well as C21,22-dehydration [12], were tentatively identified for AZA-59 in the feeding study. These AZA-59 metabolites are named AZA-73 to AZA-79 (Fig. 2, Table 2).

The elemental composition of AZA-73 was determined as $C_{47}H_{74}O_{14}N^+$ by HRMS spectrometry (Table 2), which is consistent with a hydroxylation of AZA-59. Moreover, the 23-hydroxylation of AZA-1 leading to AZA-8 results in a shift of the fragment *m/z* 462 of AZA-1 to *m/z* 478/460 of AZA-8 (Kilcoyne et al., 2015b). The same fragment pair shift was observed for AZA-73 (Fig. 3A) evidencing that AZA-73 is 23-hydroxy-AZA-59.

The elemental composition of AZA-74 was determined as $C_{47}H_{72}O_{15}N^+$ (Table 2). With two H atoms less and two additional oxygens in comparison to AZA-59, consistent with a carboxylated variant of AZA-59. This hypothesis is confirmed by the fact that AZA-74 showed two eliminations of CO_2. One elimination is typical for 3-hydroxylated AZAs that in contrast to not 3-hydroxylated AZA eliminate CO_2 via a six membered transition state including the terminal carboxylic group and the 3-hydroxylation. The first CO_2 elimination results in the *m/z* 846 fragment (Fig. 4B). A second elimination of CO_2 is evident with the *m/z* 784 fragment resulting from a loss of H_2O and two losses of CO_2 (Fig. 3B). The 22-carboxylation of AZA-1 forming AZA-17 results in a 14 Da downshift of fragment *m/z* 462 to *m/z* 448 (O'Driscoll et al., 2011), whereas fragment *m/z* 362 remains unchanged in both molecules. The same fragment pattern was also observed in the CID spectrum of AZA-74 further supporting the hypothesis that AZA-74 is 22-carboxy-AZA-59.

The elemental composition of AZA-75 was determined as $C_{46}H_{72}O_{13}N^+$ (Table 2), which corresponds to a difference of CH_2 in comparison to AZA-59. Accordingly, all *m/z* values of the fragments above *m/z* 600 are downshifted by 14 Da (Fig. 3C). Furthermore, the fragments below *m/z* 500 are shared by AZA-74 and AZA-75 indicating the same structural configuration at C22. The fact that decarboxylation of AZA-17 in mussels has been observed to occur readily leading to AZA-3 McCarron et al., 2008 especially after heating (Kilcoyne et al., 2015a), leads to the conclusion that this process also applies to AZA-59 leading to AZA-75 (22-desmethyl-AZA-59). Usually, heating is required to induce 22-decarboxylation of AZA. In this experiment samples were not heated, but hepatopancreas tissues were extracted repeatedly by reciprocal shaking, which is a high energy process and results in warming of the samples. Thus, the presence of 22-decarboxylated AZA in the samples is consistent.

AZA-76 has the elemental composition $C_{46}H_{70}O_{12}N^+$ corresponding to a loss of H_2O from AZA-75. This is equivalent to AZA-25, which formed by 21-dehydroxylation of AZA-3. The CID spectra of AZA-25 (Kilcoyne et al., 2018) and AZA-76 (Fig. 3D) match in the low mass

Table 1
Calculated number of *A. poporum* cells removed and the corresponding estimated uptake of AZA-59 by each mussel when harvested at the respective time point.

	Mussel harvest [d (h)]	Total ingestion [10^6 cells mussel^{-1}]	Total AZA-59 uptake [μg AZA-59 mussel^{-1}]
Main Experiment	0 (12)	3.8	0.7
	1 (36)	9.9	1.7
	3 (84)	27.6	5.7
Second phase	10 (258)	58.3	10.7
Final phase	17 (426)	80.0	17.1

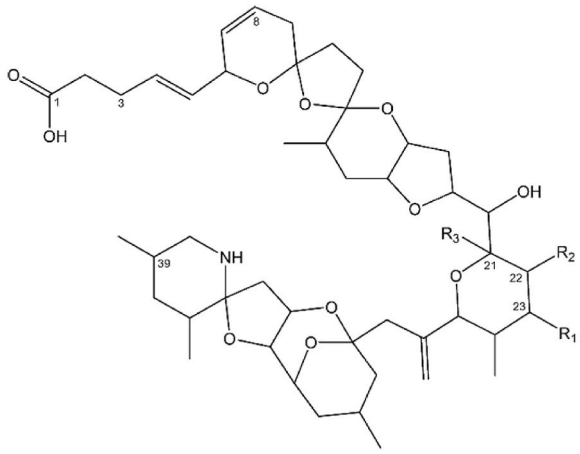

AZA	R_1	R_2	R_3 / $\Delta_{21,22}$	*m/z*
1	H	CH_3	OH / -	842
8	OH	CH_3	OH / -	858
17	H	COOH	OH / -	872
3	H	H	OH / -	828
25	H	H	H / +	810
5	OH	H	OH / -	844

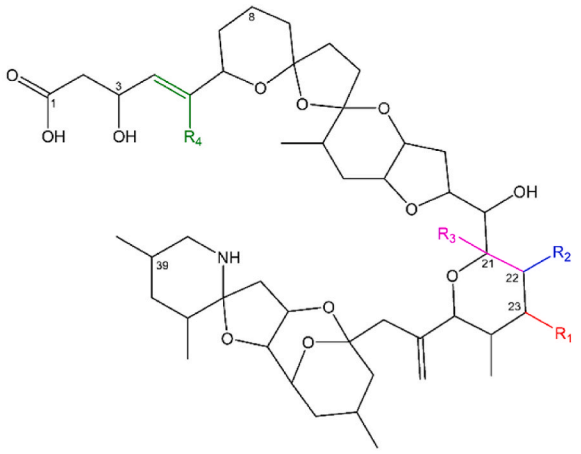

AZA	R_1	R_2	R_3 / $\Delta_{21,22}$	R_4 / $\Delta_{4,5}$	*m/z*
59	H	CH_3	OH / -	H / +	860
73	OH	CH_3	OH / -	H / +	876
74	H	COOH	OH / -	H / +	890
75	H	H	OH / -	H / +	846
76	H	H	H / +	H / +	828
77	OH	H	OH / -	H / +	862
78	H	CH_3	OH / -	OH / -	878

Fig. 2. AZA-1 (left, adapted from [12]) and AZA-59 (right) metabolites, their structures, and *m/z* values. Δ = double bond.

Table 2
Masses determined by HRMS, theoretical masses, elemental composition, and error of AZA-59 and AZA-73 to AZA-79.

Compound	Observed *m/z*	Theoretical mass	Elemental composition	±ppm
AZA-59	860.5151	860.5155	$C_{47}H_{74}O_{13}N^+$	−0.46
AZA-73	876.5100	876.5104	$C_{47}H_{74}O_{14}N^+$	−0.49
AZA-74	890.4894	890.4893	$C_{47}H_{72}O_{15}N^+$	−0.30
AZA-75	846.4995	846.4998	$C_{46}H_{72}O_{13}N^+$	−0.43
AZA-76	828.4912	828.4893	$C_{46}H_{70}O_{12}N^+$	−2.34 [a]
AZA-77	862.4758	862.4747	$C_{46}H_{72}O_{14}N^+$	−1.23 [a]
AZA-78	878.5254	878.5260	$C_{47}H_{76}O_{14}N^+$	−0.79
AZA-79	892.5063	892.5053	$C_{47}H_{74}O_{15}N^+$	−1.12 [a]

[a] Data were acquired at NRC.

fragments whereas the high mass fragments of AZA-76 are shifted to higher masses due to the lacking C7/8 double bond in the A-ring of AZA-59 and the resulting altered cleavage of a saturated A-ring in contrast to an unsaturation of the A-ring (Fig. 2). AZA-76 is only a minor compound in the relative AZA profiles of the mussel hepatopancreas.

The elemental composition of AZA-77 was determined as $C_{46}H_{72}O_{14}N^+$ (Table 2) and corresponds to AZA-59 less a methyl group and with an additional hydroxylation. Both modifications must be located in the C21-C40 part of the molecule as the *m/z* 462 fragment of AZA-59 is upshifted by 2 Da to *m/z* 464 in AZA-77 (i.e. +16 by the hydroxylation and −14 by the demethylation) (Fig. 4A) and thus is consistent with an oxidation of the 22-methyl group followed by a decarboxylation and a 23-hydroxylation. The respective AZA-1 metabolite is AZA-5.

In order to screen for other potential AZA-related compounds a precursor ion scan of the typical AZA fragment *m/z* 362 was performed. The precusor ion scan revealed the presence of two further potential precursors of *m/z* 362 with pseudomolecular ions of *m/z* 878 and *m/z* 892 that were confirmed to be AZAs by their CID spectra. The tentative structures of these AZAs, named AZA-78 (*m/z* 878) and AZA-79 (*m/z* 892), were not apparent based on the currently known AZA metabolism pathways in mussels.

AZA-78 has a pseudomolecular mass of *m/z* 878 and an elemental composition of $C_{47}H_{76}O_{14}N^+$ (Table 2), which corresponds to an addition of water to AZA-59. All fragments of AZA-78, with the exception of the molecular cluster (Fig. 4B) are identical to those of AZA-59 (Fig. 6A in Kim et al. (2017)), therefore the additional water is located in between C1 and C5. Most likely the C4/5 double bond is saturated and C4 or C5 is hydroxylated (Fig. 2). Structural confirmation based on MS is not possible due to the absence of diagnostic fragments in this region of the molecule. AZA-79 has a pseudomolecular mass of *m/z* 892 and an elemental composition of $C_{47}H_{74}O_{15}N^+$ (Table 2). This corresponds to an addition of two oxygen atoms (or hydroxylations) to AZA-59, but the mid-range fragments (*m/z* 300 to 500) of the CID spectrum of AZA-79 (Fig. 4C) are not consistent with additional hydroxylations. This is an indication that alternative alterations have occurred. The trace levels of these analogues make further investigation challenging, but should be considered in future studies.

Furthermore, in the SRM screening a few samples had peaks consistent with hypothesized transitions derived from the known metabolic pathways of AZA-1 with pseudomolecular ions at *m/z* 906, 844, and 842 that correspond to the AZA-1 metabolites AZA-44, -60, and −26, respectively. However, they were only present at trace levels that did not allow the acquisition of reasonable CID spectra (data not shown) and thus their identity as AZA metabolites cannot be confirmed.

Interestingly in a recent work Ozawa et al. (2023) fed seven species of filter feeders (clams, oysters) and ascidians with AZA-2 producing *A. poporum*, no AZA-2 metabolites were detected in any of the target species. While mussels were not tested this is strong evidence that biotransformation of phycotoxins in mollusks may be species-specific and extrapolation of phycotoxin metabolites between different mollusk species may not be possible.

3.3. Elution order of AZA-1 and AZA-59 metabolites

The elution order of AZA-59 and its detected mussel metabolites were determined with increasing retention time with the earliest eluting AZA-78 < AZA-79 < AZA-77 < AZA-74 < AZA-73 < AZA-75 < AZA-59 < AZA-76 (Fig. 5). This elution order generally reflects the degree of

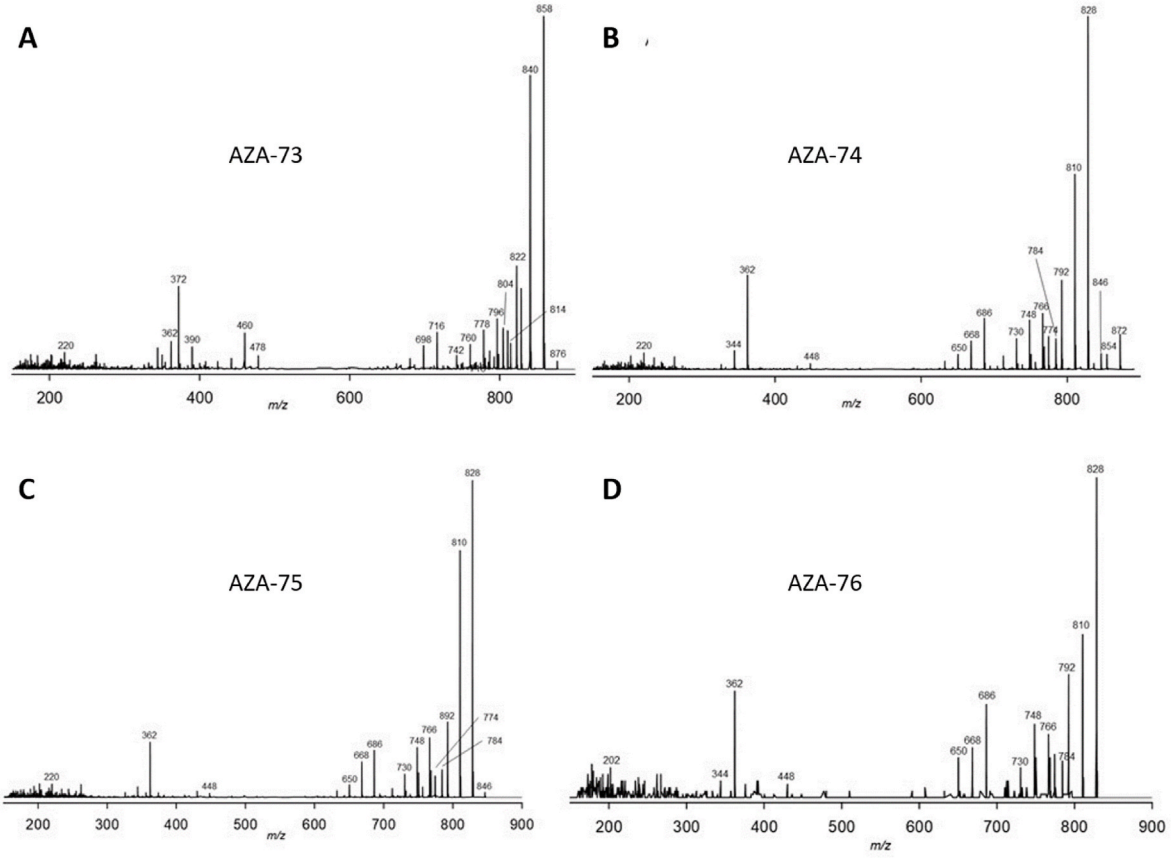

Fig. 3. CID spectra of (A) AZA-73, (B) AZA-74, (C) AZA-75, and (D) AZA-76.

oxidation, specifically the number of hydroxy groups, with the exception of AZA-74 and AZA-79.

The elution order of AZA-59 metabolites was found to be consistent with the elution order of the respective AZA-1 metabolites (Kilcoyne et al., 2018). The first eluting metabolites were those formed by C22-desmethylation and C23-hydroxylation (AZA-5/AZA-77), followed by those formed by 22-methyloxidation (AZA-17/AZA-74) and C23-hydroxylation only (AZA-8/AZA-73) (Fig. 2). The next eluting metabolite is formed by C22-desmethylation only (AZA-3/AZA-75). Relative retention times (RRT) of AZA-1 and -59 metabolites are listed in Table S5.

3.4. AZA fatty acid esters

Recent investigations highlighted the presence of fatty acid esters for C3 hydroxylated AZAs in mussels (*M. edulis*) harvested from Bruckless, Donegal Bay, Ireland (Mudge et al., 2020). Given that AZA-59 and the mussel metabolites described herein are C3 hydroxylated warranted further investigation into the presence of fatty acid esters in these hepatopancreas tissues. All-ion fragmentation LC–HRMS experiments were performed to assess the presence of AZA-ester metabolites. A chromatographic gradient with a long hold at high organic was used with fragmentation of all ions from *m/z* 100–1200, which indicated the presence of diagnostic AZA product ions at *m/z* 168.1381 and *m/z* 362.2690 (Fig. 6) eluting after the free AZAs.

Data dependent acquisition (ddMS^2) were run for each hepatopancreas tissue extract. The most prominent later eluting peak having diagnostic AZA product ions had a $[M+H]^+$ at *m/z* 1098.7467 eluting at 21.7 min, consistent with a molecular formula of $C_{63}H_{104}O_{14}N^+$ (Δ 1.6 ppm). The product ion spectrum presented a series of water losses from the $[M+H]^+$ as shown in Fig. 7. There were several diagnostic product ions observed including *m/z* 824.4938 ($C_{47}H_{70}O_{11}N^+$, Δ −0.5 ppm), which is consistent with the neutral loss of palmitic acid and one molecule of water from 3-*O*-palmitoylAZA-59 similar to the fragmentation pattern observed with 3-*O*-palmitoylAZA-4 (Mudge et al., 2020). The product ion at *m/z* 780.5039 ($C_{46}H_{70}O_9N^+$, Δ −0.6 ppm) is consistent with neutral loss of the fatty acid together with elimination of C1 as CO_2 and a subsequent loss of water. Additional diagnostic product ions at *m/z* 700.4415 ($C_{40}H_{62}O_9N^+$, Δ −0.5 ppm), and *m/z* 462.3207 ($C_{27}H_{44}O_5N^+$, Δ −0.4 ppm) are characteristic of AZA-59 cleavages occurring at the A-ring and after the D-ring, respectively (see Fig. 8).

The palmitate ester of AZA-59 was the highest abundance acyl ester across all samples and time-points, however various other fatty acid esters of AZA-59 were observed. The additional 3-*O*-acyl esters in high abundance included 18:1, 16:1, 17:0, 17:1, 20:2 and 18:0 and 14:0 based on peak area in each sample, and no significant change in fatty acid composition was observed over time (Fig. S2). The peak areas relative to 3-*O*-palmitoylAZA-59 of each derivative are summarized in Table S6.

The two most abundant AZA-59 mussel metabolites, AZA-73 and AZA-75, identified in Section 2.2 contain a 3-hydroxy group and were also metabolized into fatty acid esters in the mussel tissues. AZA-75 fatty acid esters were in higher relative abundance compared with AZA-73 esters with palmitate fatty acids being the dominant acyl esters for both. 3-*O*-palmitoylAZA-73 had an $[M+H]^+$ at *m/z* 1114.7408 corresponding to $C_{63}H_{104}O_{15}N^+$ (Δ 0.7 ppm) eluting at 15.6 min. Diagnostic product ions included *m/z* 840.4890, 796.4989, 716.4363 and 478.3159 (Fig. 9A). AZA-73 contains a 23-hydroxy group and evidence of this is the cross-ring cleavage occurring at ring E resulting in the product ion at *m/z* 372.2529. The presence of these ions confirms this ester to have the backbone of AZA-73. 3-*O*-palmitoylAZA-75, eluting at 19.4 min, had an $[M+H]^+$ at *m/z* 1084.7314 corresponding to $C_{62}H_{102}O_{14}N^+$ (Δ 1.9 ppm). Diagnostic product ions including *m/z* 810.4780, 766.4883, 686.4258 and 448.3054 (Fig. 9B) confirmed this backbone to be AZA-

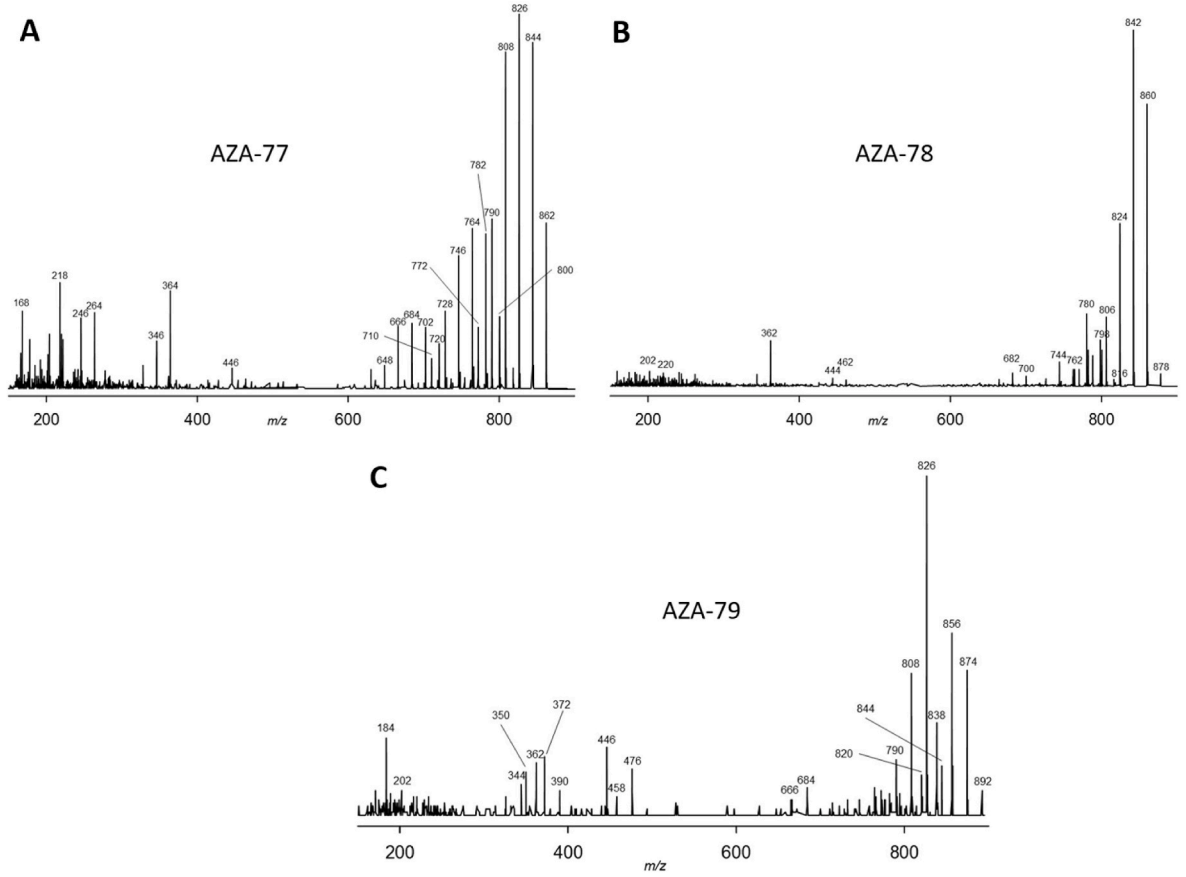

Fig. 4. CID spectra of (A) AZA-77, (B) AZA-78, and (C) AZA-79.

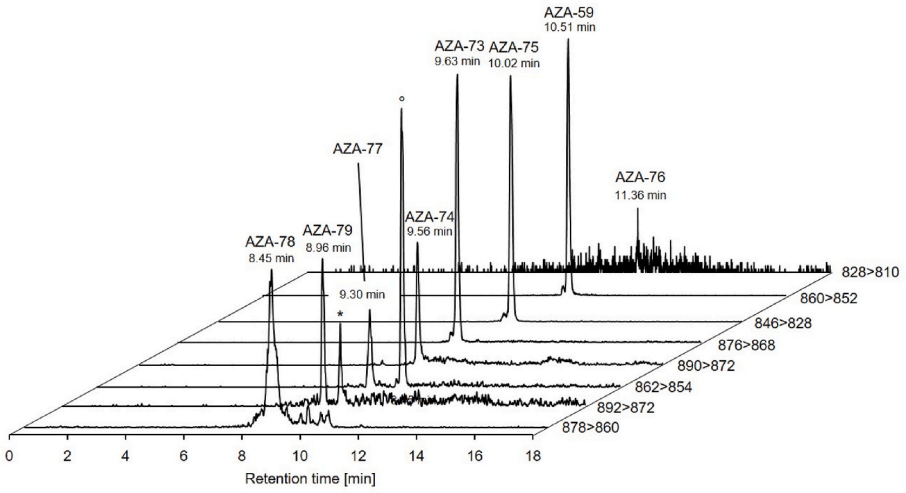

Fig. 5. Extracted ion chromatograms of AZA-59 and its metabolites found in this study. AZAs are in the order of increasing retention times. * = isotopic satellite of AZA-74; ° = isotopic satellite of AZA-59.

75. Several additional fatty acid acyl esters, including 18:1, 16:1, 17:0 and 22:6, were observed for AZA-73 and AZA-75.

Trace levels of fatty acid acyl esters of several additional AZA-59 metabolites, primarily as palmitoyl esters, were observed in the tissues and were more prevalent in the mussels exposed to *A. poporum* for longer time periods. Two appear to be consistent with the trace mussel metabolites AZA-77 and AZA-78. Additionally, analysis of the residual mussel tissue extracted with methanol and analyzed directly confirmed the presence of fatty acid acylated AZA-74 in high abundance (Fig. S3). Appreciable levels of these carboxylated compounds were not observed in the hepatopancreas tissue extracts due to decarboxylation during sample handling and/or storage prior to LC–HRMS analysis.

3.5. Formation and distribution of AZA metabolites

The dominant AZA variant, excluding esters, in all experimental samples including the mussel tissues, the aquarium water, and particulate residues in the aquaria was the unmetabolized AZA-59. The most

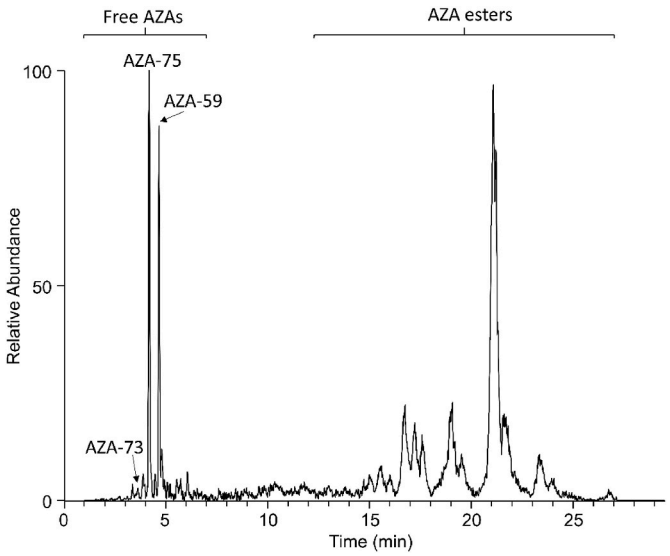

Fig. 6. Extracted ion chromatogram of AZA diagnostic ions at *m/z* 168.1381 and *m/z* 362.2690 with a ±5 ppm mass tolerance collected using an all-ion fragmentation of the mass range of *m/z* 100 to 1200 of a 426-h feeding mussel hepatopancreas extract from the *A. poporum* mussel feeding study.

abundant metabolite, excluding esters, found in the hepatopancreas tissues was 22-desmethyl-AZA-59 (AZA-75). However, the relative proportion of AZA-75 in relation to AZA-59 did not change much except for the last sampling point after 426 h where AZA-75 reached the same level as AZA-59 (Fig. 9). The intermediate 22-carboxy-AZA-59 (AZA-74) was only detected at trace levels in the hepatopancreas tissues most likely due to decarboxylation during sample handling prior to analysis.

The second most abundant non-esterified AZA-59 metabolite in the hepatopancreas was 23-hydroxy-AZA-59 (AZA-73), which did not exceed 10% of AZA-75 (Fig. 9A). All other non-esterified AZA-59 metabolites were only detected at trace levels. The same trend was found in the aquarium water and residues with AZA-75 being the most abundant non-esterified metabolite, however at lower proportion than in the hepatopancreas (Fig. 9B). AZA-75 is formed from AZA59, via oxidation of the C22 methyl group and subsequent decarboxylation. This is equivalent to AZA-3 which has been proven to be the decarboxylation product of AZA-17, which in turn is formed by oxidation of the methyl group at C22 of AZA-1 (O'Driscoll et al., 2011). Decarboxylation has been shown to be a heat-induced reaction (Kilcoyne et al., 2015a) and unheated samples usually contain a higher proportion of carboxylated vs. decarboxylated variants. The relatively high proportion of AZA-75 and low levels of AZA-74 (22-carboxy-AZA-59) not exceeding 1% of total unesterified AZA can be explained by the extraction with ceramic beads at high speed, which leads to warming of the samples. Direct analysis of the methanolic extracts of residual mussel tissues extracted without the addition of ceramic beads showed high levels of AZA-74 and its acyl esters, suggesting that decarboxylation may have occurred when preparing the hepatopancreas tissues extracts. It is also interesting that the relative profiles do not change much during the 18-day experiment indicating a metabolic turnover that is in the same order of magnitude of the uptake of new AZA-59 in the course of the experiment. Interestingly, the proportion of AZA-59 in the AZA profiles of the particulate matter and water of the aquaria was far higher than in hepatopancreas (Fig. 9A/B) indicating that AZA-59 is passed into the environment by either rapid passage of AZA-59 through the digestive glands of mussels without modification and/or by crushing delicate *Azadinium* cells during the filtration process.

AZA-76 (21,22-dehydro-21-dehydroxy-22-desmethyl-AZA-59), and AZA-77 (23-hydroxy-22-desmethyl-AZA-59) were detected at very low proportions and at later time points of the experiments. Even though the pathways leading to these metabolites do not seem to play a major role and only contribute to low total AZA content in mussels, their formation clearly shows that the metabolic activity of mussels acts in the same way on AZA-1 as on AZA-59.

AZA acyl esters were dominated by those with AZA-59 backbones, which accounted for between 64 % at 12 h and 83 % at 426 h (data not shown) of the total AZA acyl ester content. As noted previously, acylated AZA-75 metabolites were in higher abundance than acylated AZA-73 metabolites, suggesting that AZA-59 may readily form acyl esters in the hepatopancreas following ingestion, and possibly at a faster rate compared with the biotransformation of AZA-59 into other free

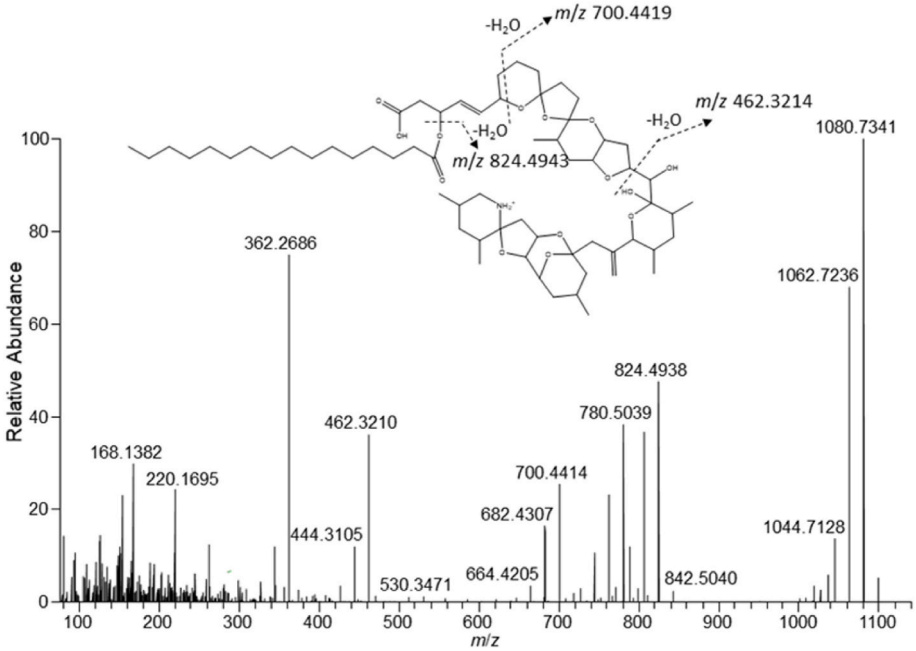

Fig. 7. Product ion spectrum of the most abundant AZA-acyl ester present in the mussels fed *A. poporum* with an $[M+H]^+$ at *m/z* 1098.7459 and product ions consistent with 3-*O*-palmitoylAZA-59 with a scheme showing the proposed origins of the major diagnostic ions with exact masses.

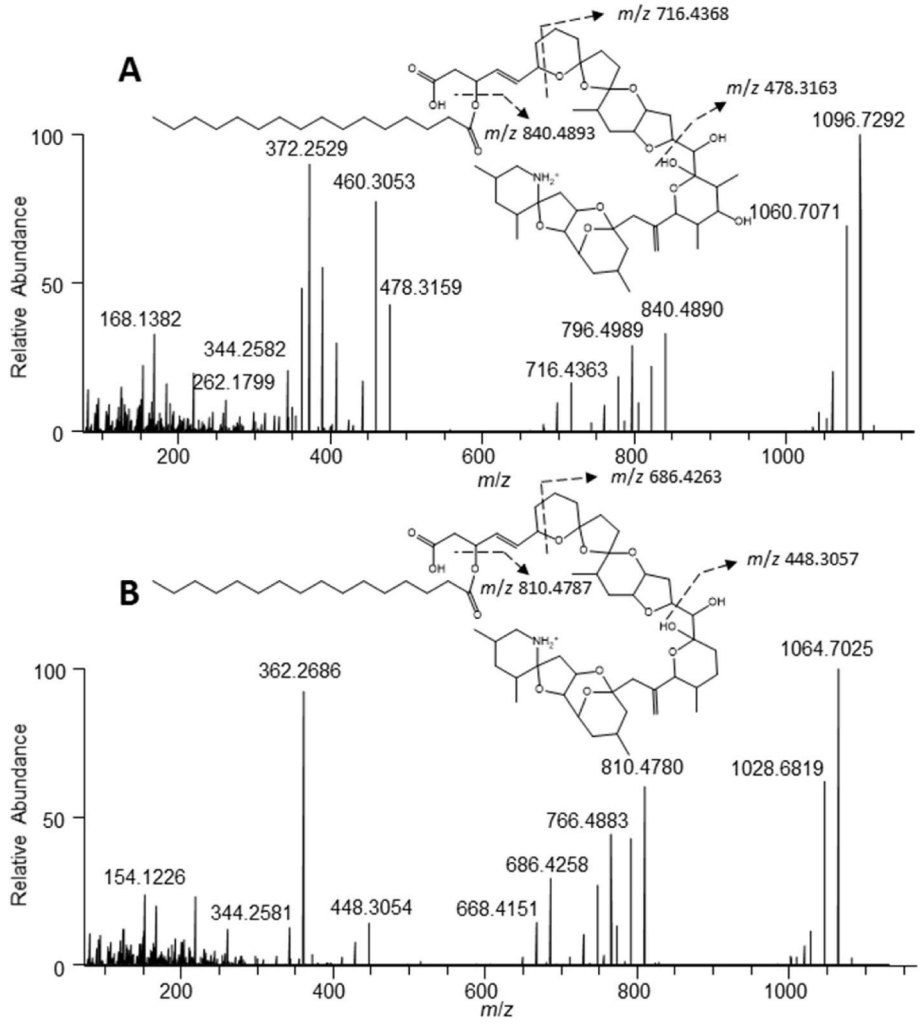

Fig. 8. Product ion spectra of palmitate acyl esters of (A) AZA-73 and (B) AZA-75 obtained using ddMS^2 acquisition on the mussel hepatopancreas tissues collected during the feeding study with *A. poporum*.

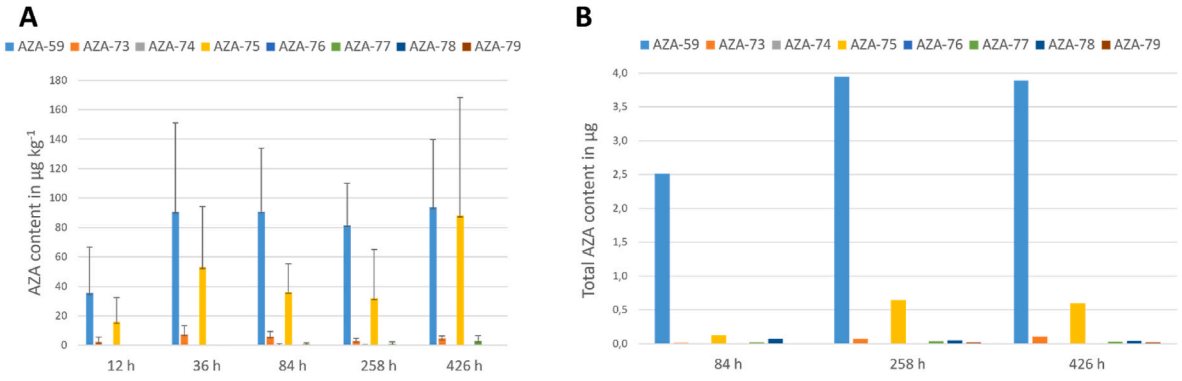

Fig. 9. Toxin profiles of (A) hepatopancreas (expressed as µg kg^{-1} HP) after 12, 36, 84, 258, and 426 h determined in triplicates and of (B) aquarium water and residues after 84, 258, and 426 h (expressed as total AZA amount in µg).

analogues. Comparison of the average free and acylated AZAs (in µg kg^{-1}) in the hepatopancreas over the course of the feeding study also indicates that the major proportion of AZAs are metabolized into acyl esters, which increase in content over time (Fig. 10). The ratio of AZA-esters to free AZAs increases from 3:1 at 12 h to 23:1 at 426 h.

AZA-59 contains a C3-hydroxy group, similar to the AZA-1 metabolite AZA-4, which was the backbone structure of the majority of previously identified fatty acid esters in European mussels while acylation was not observed for the other hydroxyl groups of the major AZAs (Mudge et al., 2020). AZA-59 was rapidly esterified and those fatty acid esters accumulated in the mussel tissues throughout the time course of this feeding study. Previous feeding studies with *A. spinosum* investigating accumulation of AZA-1 and AZA-2 and related metabolites did not consider the formation of esters (Jauffrais et al., 2012a, 2012c).

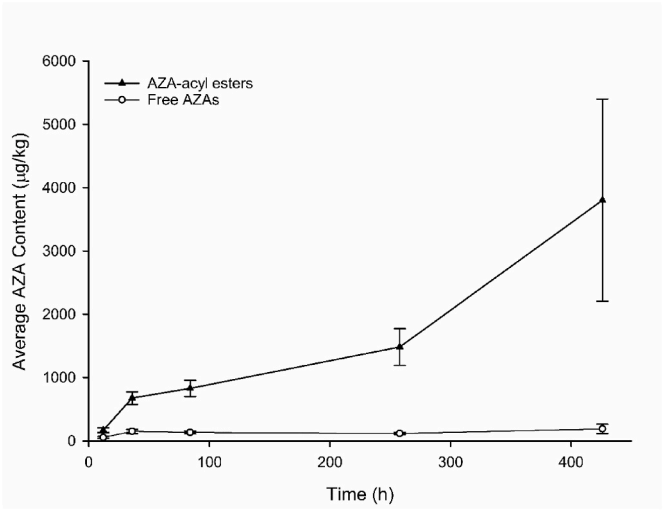

Fig. 10. Average AZA content of non-esterified AZA and fatty acid acylated AZA in mussel hepatopancreas tissues during the time course of the feeding study. AZA content is estimated based on AZA-1 equivalents. Error bars represent standard error of the mean (SE).

Short term feedings (4–7 d) highlighted that the levels of free AZAs remained consistent throughout the study (Jauffrais et al., 2012a, 2012c), and extrapolation of this data to other studies suggests there may be additional storage pathways such as fatty acid esterification leading to significantly higher accumulation of AZAs in the tissues. This would require future work to monitor the accumulation and depuration of AZA metabolites including fatty acid esters.

3.6. AZA uptake, accumulation, and mass balance estimate

In order to assess the fate of AZA-59 over the course of the feeding experiment, AZA-59 was determined in the *A. poporum* cultures fed to the mussels. AZA-59 and its metabolites were assessed in several experimental compartments including mussel hepatopancreas tissues, fecal pellets, particulate matter of the aquaria and dissolved toxins in the aquaria water following mussel harvest and at the end of the entire experiment. As shown in Fig. 1C, mussels constantly cleared and fed on *A. poporum* during the experiment and the estimated uptake of AZA-59 increased from 0.7 µg mussel^{-1} after 12 h up to 17.1 µg mussel^{-1} after 426 h (Table 1).

In contrast to the continuous removal of *A. poporum* cells (indicating a continuous uptake of AZA-59), the average total free AZA in mussel hepatopancreas plateaued (Table S7). The content of total acylated AZA in the mussel hepatopancreas continued to increase through the entire experiment. For the study of AZA metabolites, AZAs were only measured in the hepatopancreas tissues and thus it is not possible to quantitate total AZA content (µg kg^{-1}) in the mussels accurately. However, the hepatopancreas-free mussel flesh of three mussels was tested and only very low amounts of free AZAs (<0.1% of hepatopancreas levels) were detected (Table 3 and S8). The hepatopancreas level of free AZAs (excluding esters) hardly exceeded 200 µg kg^{-1}. Considering that on average the hepatopancreas tissue made up less than 10% of total mussel soft tissue (Table S2), the free AZA content is estimated at approximately 20 µg kg^{-1} in total mussel soft tissues in this feeding experiment. The analysis of free AZAs in the samples taken during the experiment and in the remaining experimental compartments after the completion of the feeding study revealed that only a low percentage (0.9 %) of all ingested AZA-59 was present as free AZA-59 in the mussel hepatopancreas, whereas the remaining mussel tissues contained very low amounts (Table 3). Notably, the estimate of AZA-esters in the hepatopancreas was 6.5 µg, more than six times higher than free AZAs. A small subset of mussel flesh samples (following removal of the hepatopancreas) were evaluated for the presence of AZA-esters, and showed the ratio of AZA-esters to free AZAs was relatively consistent with that observed in the hepatopancreas. Due to this limited sample subset and complexity of extrapolating an estimate of total AZAs across the residual mussel tissues, it was not possible to estimate the total AZA content present as acyl esters in residual tissues. In summary, approximately 7% of AZA-59 introduced during the experiment from the algae was estimated in mussel tissues in the form of AZA-59, non-esterified AZA metabolites or as AZA-esters. An additional 14% of the total introduced AZA was estimated in compartments outside the animals including the aquarium water (4.7%) and aquaria water particulate residues (fecal pellets, detritus, etc.; 9.3 %) (Table 3). Combined, this accounts for an estimate of approximately 21% of the total AZA-59 introduced during the mussel feeding experiment. While the primary objective of this work was to understand the formation of AZA-59 metabolites in mussels, this discrepancy between introduced AZA-59 and the total estimate of AZA-59 metabolites is interesting and merits consideration as part of future studies. Acknowledging that these numbers are semi-quantitative estimates, and accepting the challenges with extrapolations between tissue compartments as described above, there are a number of other quantitative analytical considerations to bear in mind. The extraction efficiency from different tissues and samples may vary significantly. Another factor is that all AZA values were expressed as AZA-1 equivalents due to the lack of individual standards for the newly identified compounds, where relative response factors of these individual AZAs compared to AZA-1 in the mass spectrometer are unknown. Sample matrix effects causing ionization suppression can also introduce significant biases: AZA inputs were estimated based on analysis of algal extracts, while recovery was based on mussel hepatopancreas extracts, where varying sample matrix effects may impact quantitation between these sample types. In addition to these analytical factors, this experiment only detected AZAs with a conserved carbon skeleton. AZA metabolites with additional modifications of the AZA backbone could further affect the overall recovery estimates.

Table 3
Estimates of AZA distribution in relation to total AZA-59.

AZA fraction	Absolute amount [µg]	Percentage of total added AZA-59 (%)
Total AZA-59 from *A. poporum*	105	100
Free AZA of hepatopancreas	0.9	0.9
AZA-ester of hepatopancreas	6.5	6.2
Free AZA in mussel flesh (without hepatopancreas)	0.006[a]	0.006
Total AZA content in mussels	**7.4**	**7.0**
Free AZA dissolved in aquarium water	4.9	4.7
Free AZA particulate in aquarium water	9.8	9.3
Total free AZA in aquarium water	**14.7**	**14.0**
Total AZA	**22.1**	**21.0**

[a] values extrapolated from three individuals.

4. Conclusions

This study indicates that *A. poporum* is readily ingested and AZA-59 is accumulated by mussels under controlled conditions. AZA-59 metabolized into a variety of analogues that directly match the metabolic pathway of AZA-1. Given that it is the only AZA variant in the NE Pacific highlights the need to investigate the occurrence of these analogues in naturally incurred tissues as it may suggest additional regulatory measures for other AZAs outside of AZA-1, -2, and -3 in order to protect shellfish consumers. Furthermore, there is an urgent need for reference material of AZA-59 to enable accurate and precise quantification of the

AZA-59 load of contaminated seafood.

The accumulation and metabolism of AZA-59 into its related metabolites and esters has not been verified in naturally incurred samples. Future work evaluating the presence of AZA-59 accumulation in shellfish and metabolism during *A. poporum* blooms may provide additional evidence of the metabolic transformation of AZA-59 in nature and how it relates to environmental monitoring, food safety, and toxicology. While little is known on the accumulation of AZA esters in naturally incurred mussel tissues, the large proportion of AZA-esters observed throughout this feeding study suggests monitoring acylated AZAs should be considered when assessing total toxin quotas in the mussels as a significant level of accumulation may occur. Future work will also need to consider both the toxicological significance of acylated AZAs, and the possibility that they may undergo hydrolysis following ingestion leading to higher than expected levels of free AZAs.

Supplementary Materials: Fig. S1: Cell density changes and corresponding filtration rates during the extended exposure periods, Fig. S2: Average fatty acid proportions for AZA-59 acyl esters in the mussel hepatopancreas tissues throughout the time course feeding study, Fig. S3: Product ion spectrum of the 3-O-palmitoylAZA-74, Table S1: Time points, mean AZA-59 cell quotas of *A. poporum* cultures, Table S2: Harvest dates, mussel size, and weight of mussel tissues, Table S3: Selected reaction monitoring (SRM) transitions monitored for AZAs in this study, Table S4: Ingestion rates (10^6 *A. poporum* cells per mussel per hour), Table S5: Relative Retention Times of AZA-1 and AZA-59 metabolites, Table S6: Accurate masses (for $[M+H]^+$), retention times and average relative abundances of AZA-59 fatty acid acyl esters to 3-*O*-palmitoyl AZA-59 detected in the mussel hepatopancreas tissues during the feeding study with *A. poporum*, Table S7: Time dependent mean AZA content in the mussel hepatopancreas tissues, Table S8: Total free AZA in HP-free mussel flesh.

Ethical satetement

The authors declare that all animal experiments were conducted in compliance with the EU Directive 2010/63/EU for animal experiments. Approvals for experiments with mussels are not required by the EU Directive.

CRediT authorship contribution statement

Bernd Krock: Writing – review & editing, Writing – original draft, Investigation, Data curation, Conceptualization. **Elizabeth M. Mudge:** Writing – review & editing, Investigation, Data curation, Conceptualization. **Annegret Müller:** Methodology, Investigation. **Stefanie Meyer:** Methodology, Investigation. **Jan Tebben:** Methodology, Investigation. **Pearse McCarron:** Writing – review & editing, Conceptualization. **Doris Abele:** Conceptualization. **Urban Tillmann:** Writing – review & editing, Methodology, Investigation, Data curation, Conceptualization.

Funding

This research was funded by the Helmholtz-Gemeinschaft Deutscher Forschungszentrum through the research program “Changing Earth - Sustaining our Future” of the Alfred-Wegener-Institut Helmholtz-Zentrum für Polar-und Meeresforschung.

Declaration of competing interest

The authors declare that they have no known competing financial interests or personal relationships that could have appeared to influence the work reported in this paper.

Acknowledgments

We thank Vera Trainer (University of Washington) and the MERHAB program, Brian Bill (NOAA) and Joo-Hwan Kim (Hanyang University) for providing and maintaining the sediment samples from Puget Sound needed to isolate the *Azadinium* strain 121-E10. We thank Luisa Hintze for partial SRM measurements of shellfish samples in the frame of a student internship.

Appendix A. Supplementary data

Supplementary data to this article can be found online at https://doi.org/10.1016/j.toxicon.2024.108152.

Data availability

Data will be made available on request.

References

Frost, B., 1972. Effects of size and concentration of food particles on the feeding behavior of the marine planktonic copepod *Calanus pacificus*. Limnol. Oceanogr. 17, 805–815.
James, K., Furey, A., Satake, M., Yasumoto, T., 2000. Azaspiracid poisoning (AZP): a new shellfish toxic syndrome in Europe. In: 9th International Conference on Harmful Algae Blooms, Hobart, Australia.
Jauffrais, T., Contreras, A., Herrenknecht, C., Truquet, P., Séchet, V., Tillmann, U., Hess, P., 2012a. Effect of *Azadinium spinosum* on the feeding behaviour and azaspiracid accumulation of *Mytilus edulis*. Aquat. Toxicol. 179–187.
Jauffrais, T., Herrenknecht, C., Séchet, V., Sibat, M., Tillmann, U., Krock, B., Kilcoyne, J., Miles, C.O., McCarron, P., Amzil, Z., Hess, P., 2012b. Quantitative analysis of azaspiracids in *Azadinium spinosum* cultures. Anal. Bioanal. Chem. 403, 833–846.
Jauffrais, T., Marcaillou, C., Herrenknecht, C., Truquet, P., Séchet, V., Nicolau, E., Tillmann, U., Hess, P., 2012c. Azaspiracid accumulation, detoxification and biotransformation in blue mussels (*Mytilus edulis*) experimentally fed *Azadinium spinosum*. Toxicon 60, 582–595.
Ji, Y., Qiu, J., Xie, T., McCarron, P., Li, A., 2018. Accumulation and transformation of azaspiracids in scallops (*Chlamys farreri*) and mussels (*Mytilus galloprovincialis*) fed with *Azadinium poporum*, and response of antioxidant enzymes. Toxicon 143, 20–28.
Keller, M.D., Selvin, R.C., Claus, W., Guillard, R.R.L., 1987. Media for the culture of oceanic ultraphytoplankton. J. Phycol. 23, 633–638.
Kilcoyne, J., Nulty, C., Jauffrais, T., McCarron, P., Herve, F., Foley, B., Rise, F., Crain, S., Wilkins, A.L., Twiner, M.J., Hess, P., Miles, C.O., 2014. Isolation, structure elucidation, relative LC-MS response, and *in vitro* toxicity of azaspiracids from the dinoflagellate *Azadinium spinosum*. J. Nat. Prod. 77, 2465–2474.
Kilcoyne, J., McCarron, P., Hess, P., Miles, C.O., 2015a. Effects of heating on proportions of azaspiracids 1–10 in mussels (*Mytilus edulis*) and identification of carboxylated precursors for azaspiracids 5, 10, 13, and 15. J. Agric. Food Chem. 63, 10980–10987.
Kilcoyne, J., Twiner, M.J., McCarron, P., Crain, S., Giddings, S.D., Foley, B., Rise, F., Hess, P., Wilkins, A.L., Miles, C.O., 2015b. Structure elucidation, relative LC–MS response and *in vitro* toxicity of azaspiracids 7–10 isolated from mussels (*Mytilus edulis*). J. Agric. Food Chem. 63, 5083–5091.
Kilcoyne, J., McCarron, P., Twiner, M.J., Rise, F., Hess, P., Wilkins, A.L., Miles, C.O., 2018. Identification of 21,22-dehydroazaspiracids in mussels (*Mytilus edulis*) and *in vitro* toxicity of azaspiracid-26. J. Nat. Prod. 81, 885–893.
Kim, J.-H., Tillmann, U., Adams, N.G., Krock, B., Stutts, W.L., Deeds, J.R., Han, M.-S., Trainer, V.L., 2017. Identification of *Azadinium* species and a new azaspiracid from *Azadinium poporum* in Puget Sound, Washington state, USA. Harmful Algae 68, 152–167.
Krock, B., Tillmann, U., John, U., Cembella, A.D., 2009. Characterization of azaspiracids in plankton size-fractions and isolation of an azaspiracid-producing dinoflagellate from the North Sea. Harmful Algae 8, 254–263.
Krock, B., Tillmann, U., Witt, M., Gu, H., 2014. Azaspiracid variability of *Azadinium poporum* (dinophyceae) from the China Sea. Harmful Algae 36, 22–28.
Krock, B., Tillmann, U., Potvin, É., Jeong, J.H., Drebing, W., Kilcoyne, J., Al-Jorani, A., Twiner, J.M., Göthel, Q., Köck, M., 2015. Structure elucidation and *in vitro* toxicity of new azaspiracids isolated from the marine dinoflagellate *Azadinium poporum*. Mar. Drugs 13, 6687–6702.
Krock, B., Tillmann, U., Tebben, J., Trefault, N., Gu, H., 2019. Two novel azaspiracids from *Azadinium poporum*, and a comprehensive compilation of azaspiracids produced by Amphidomataceae, (Dinophyceae). Harmful Algae 82, 1–8.
McCarron, P., Kilcoyne, J., Miles, C.O., Hess, P., 2008. Formation of Azaspiracids-3, -4, -6, and -9 via Decarboxylation of Carboxyazaspiracid Metabolites from Shellfish. J. Agricult. Food Chem. 57/1, 160–169.
McMahon, T., Silke, J., 1996. West coast of Ireland; winter toxicity of unknown aetiology in mussels. Harmful Algae News 14, 2.
Mudge, E.M., Miles, C.O., Hardstaff, W.R., McCarron, P., 2020. Fatty acid esters of azaspiracids identified in mussels (*Mytilus edulis*) using liquid chromatography-high resolution mass spectrometry. Toxicon, 100059.
Ozawa, M., Uchida, H., Watanabe, R., Matsushima, R., Oikawa, H., Takahashi, K., Iwataki, M., Suzuki, T., 2023. Azaspiracid accumulation in Japanese coastal bivalves and ascidians fed with *Azadinium poporum* producing azaspiracid-2 as the dominant toxin component. Toxicon 226, 107069.

O'Driscoll, D., Škrabáková, Z., O'Halloran, J., van Pelt, F.N.A.M., James, K.J., 2011. Mussels increase xenobiotic (azaspiracid) toxicity using a unique bioconversion mechanism. Environ. Sci. Technol. 45, 3102–3108.

Ramírez, F.J., Guinder, V.A., Ferronato, C., Krock, B., 2022. Increase in records of toxic phytoplankton and associated toxins in water samples in the Patagonian Shelf (Argentina) over 40 years of field surveys. Harmful Algae 118, 102317.

Rossi, R., Dell'Aversano, C., Krock, B., Ciminiello, P., Percopo, I., Tillmann, U., Soprano, V., Zingone, A., 2017. Mediterranean *Azadinium dexteroporum* (Dinophyceae) produces six novel azaspiracids and azaspiracid-35: a structural study by a multi-platform mass spectrometry approach. Anal. Bioanal. Chem. 409, 1121–1134.

Salas, R., Tillmann, U., John, U., Kilcoyne, J., Burson, A., Cantwell, C., Hess, P., Jauffrais, T., Silke, J., 2011. The role of *Azadinium spinosum* (Dinophyceae) in the production of azaspiracid shellfish poisoning in mussels. Harmful Algae 10, 774–783.

Tebben, J., Zurhelle, C., Tubaro, A., Samdal, I.A., Krock, B., Kilcoyne, J., Sosa, S., Trainer, V.L., Deeds, J.R., Tillmann, U., 2023. Structure and toxicity of AZA-59, an azaspiracid shellfish poisoning toxin produced by *Azadinium poporum* (Dinophyceae). Harmful Algae 124, 102388.

Tillmann, U., Elbrächter, M., Krock, B., John, U., Cembella, A., 2009. *Azadinium spinosum* gen. et sp. nov. (Dinophyceae) identified as a primary producer of azaspiracid toxins. Eur. J. Phycol. 44, 63–79.

Tillmann, U., Borel, C.M., Barrera, F., Lara, R., Krock, B., Almandoz, G.O., Witt, M., Trefault, N., 2016. *Azadinium poporum* from the Argentine continental shelf, Southwestern Atlantic, produces azaspiracid-2 and azaspiracid-2 phosphate. Harmful Algae 51, 40–55.

Tillmann, U., Jaén, D., Fernández, L., Gottschling, M., Witt, M., Blanco, J., Krock, B., 2017. *Amphidoma languida* (Amphidomatacea, Dinophyceae) with a novel azaspiracid toxin profile identified as the cause of molluscan contamination at the Atlantic coast of southern Spain. Harmful Algae 62, 113–126.

Tillmann, U., Edvardsen, B., Krock, B., Smith, K.F., Paterson, R.F., Voß, D., 2018. Diversity, distribution, and azaspiracids of Amphidomataceae (Dinophyceae) along the Norwegian coast. Harmful Algae 80, 15–34.

Trainer, V.L., King, T.L., 2023. SoundToxins: a research and monitoring partnership for harmful phytoplankton in Washington state. Toxins 15, 189.

USDA (United States Department of Agriculture), 2013. Census of Aquaculture (Volume 3, Special Studies, Part 2 No. AC-12-SS-2). USDA, Washington, DC, USA, p. 98p.